Performance Analysis of Reuse Partitioning Techniques in OFDMA based Cellular Radio Networks

Zheng Xie and Bernhard Walke
Communication Networks (ComNets) Research Group
RWTH Aachen University
Aachen, Germany
{tao|walke}@comnets.rwth-aachen.de

Abstract— **Reuse partitioning is a useful method for mitigating co-channel interference (CCI) in orthogonal frequency division multiple access (OFDMA) based cellular environments. In this work, theoretical analysis of a series of reuse partitioning approaches is carried out, which contains the well-known Soft Frequency Reuse (SFR) scheme, the novel Enhanced Fractional Frequency Reuse (EFFR) scheme and two EFFR-derivatives, namely the EFFR-Advanced scheme and the EFFR-Beyond scheme. Based on the Carrier to Interference plus Noise Ratio (CINR) computation, we give the maximal cell radius and reasonable boundary definitions for division different user-type zones by using each of these reuse partitioning schemes. Through numerical evaluations, cell coverage and mean cell capacity of these schemes under two different propagation conditions are exhibited. The results show that the EFFR series can outperform the SFR and the conventional reuse schemes under any propagation mode. Furthermore, among all EFFR schemes, the EFFR-Advanced scheme with an adequate resource allocation may be the best solution for CCI mitigation, which can achieve not only the 100% cell coverage but also significant cell capacity enhancement.**

Keywords - performance analysis; interference mitigation; frequency reuse; reuse partitioning; OFDMA; cellular networks

I. INTRODUCTION

Co-channel interference (CCI) mitigation is always a big challenge issue in cellular networks. In the previous work [5], we have proposed an Enhanced Fractional Frequency Reuse (EFFR) scheme with an interference-aware reuse mechanism to achieve not only CCI limitation at cell edge but also enhancement of overall cell capacity in orthogonal frequency division multiple access (OFDMA) based communication networks. Performance comparison among the EFFR, the well-known Soft Frequency Reuse (SFR) scheme [2], as well as two classical reuse schemes by extensive system-level simulations has also been contributed in that work. In this work, we will further propose other two reuse partitioning techniques, which are advanced based on the EFFR scheme, and present performance analysis of the EFFR series and the SFR scheme. With the usage of Carrier to Interference plus Noise Ratio (CINR) calculation, the maximal cell radius and reasonable boundary definitions for division different user-type zones for each reuse partitioning scheme will be given. Furthermore, through numerical evaluations, the cell coverage and the mean cell capacity of all studied reuse techniques will be estimated and compared.

II. REUSE PARTITIONING TECHNIQUES TO MITIGATE CO-CHANNEL INTERFERENCE

Reuse partitioning is one of the effective methods for attaining both coverage and higher system capacity in multi-cell environments [1]-[5]. According to different frequency reuse manner, they can be distinguished in two categories, namely, *inclusive* and *exclusive* reuse partitioning. In the following presented schemes, the SFR is an inclusive reuse partitioning scheme, whereas the EFFR series belongs to the exclusive reuse partitioning techniques.

A. Soft Frequency Reuse

The Soft Frequency Reuse (SFR) scheme [2], which has been adopted in the 3GPP-LTE system, alleviates CCI from the neighboring cells by increasing Frequency Reuse factor (FRF) and transmission power for the cell-edge users, and thereby to improve their performance and enhance the system capacity.

The basic idea of the SFR scheme is applying FRF of 1 to cell-centre users (CCU) and FRF of 3 to cell-edge user (CEU) as illustrated in Fig. 1. Simply one third of the whole available bandwidth named *Major Segment* can be used by the CEUs with higher power. To actualize FRF of 3 for the CEUs, Major Segments among directly adjoining cells should be orthogonal. In opposite to the CEUs, the CCUs may access the entire frequency resources, yet with lower transmission power to avoid yielding excessive CCI to the co-channel users in the

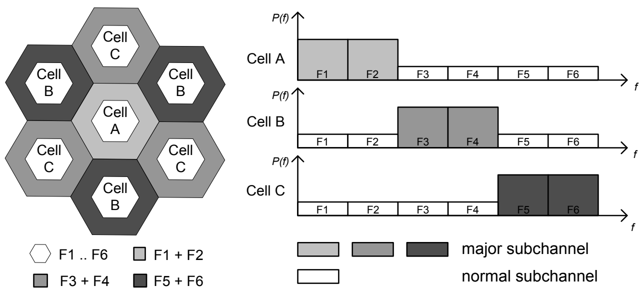

Fig. 1. Concept of the SFR scheme in a cellular system based on FRF of 3 for CEUs and FRF of 1 for CCUs.

adjacent cells. The SFR applies an *inclusive* reuse partitioning, since the Major Segment (FRF of 3) for the CEUs in a cell is simultaneously reuse-1 subchannels used by CCUs in the neighboring cells.

B. *Enhanced Fractional Frequency Reuse*

In work [5], the detailed EFFR architecture has been elaborated. The objective of the EFFR scheme is to improve system capacity while bettering spectrum efficiency at the cell edge.

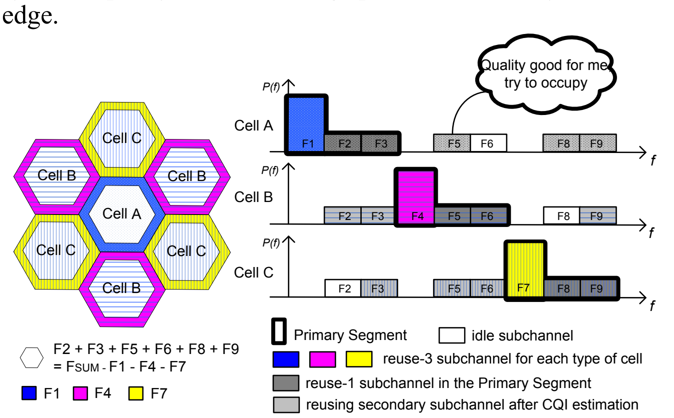

Fig. 2. Concept of the EFFR scheme in a cellular system based on exclusive partition of reuse-3 subchannels and reuse-1 subchannels in the Primary Segment, as well as interference-aware reuse on the Secondary Segment.

The EFFR scheme divides the whole available bandwidth into a *Primary Segment* and a *Secondary Segment* as shown in the right part of Fig. 2. The *exclusive* reuse-3 subchannels in the Primary Segment will be preferentially used by CEUs with higher transmission power, whereas the remaining subchannels are all reuse-1 subchannels allowing to be used by CCUs with lower power. Exclusive reuse implies the reuse-3 subchannels cannot be reused by directly neighboring cells, which decreases the CCI for the vulnerable CEUs. As each kind of station has a constant total transmission power, and any cell-type (e.g., cell-type-A in Fig. 2) is not allowed to use the reuse-3 subchannels dedicated to the other two cell-types (e.g., cell-type-B and -C in Fig. 2), the power allotted to the reuse-3 subchannels can be tripled without decreasing the transmission power for the other available reuse-1 subchannels.

In addition, the resources in the Secondary Segment will be occupied by means of Signal-to-Interference-Plus-Noise-Ratio (SINR) estimation. That means each cell can occupy all subchannels of its Primary Segment at will, whereas only a part of subchannels in the Secondary Segment can be used by this cell in an interference-aware manner.

It should be noted that some factors play paramount roles in the EFFR design and could influence the system performance severely, for example: the number of reuse-3 subchannels M and reuse-1 subchannels N in the Primary Segment; the power ratio of the high power level to the low power level; the boundary definition for partitioning the CCUs and the CEUs; the SINR threshold for reuse in the Secondary Segment etc.. In section III and IV, based on a numerical calculation of the carrier-to-interference values, we will give the boundary definition for division CCU-zone and CEU-zone for both EFFR scheme and SFR scheme. Furthermore, in section VI, by deriving the mean reachable cell capacity, reasonable numbers of subchannels M and N will also be revealed.

C. *Enhanced Fractional Frequency Reuse - Advanced*

In order to further promote the performance of the most distant users, which are located near the cell border, an Enhanced Fractional Frequency Reuse – Advanced (EFFR-A) scheme is proposed. Based on the EFFR, the EFFR-A scheme further separates the CEUs into cell-middle users (CMU) and cell-remote users (CRU). For the CRUs, the EFFR-A enlarges the co-channel distance and possibly increases the transmission power on their subchannels. Fig. 3 illustrates the EFFR-A design in a cellular system up to 3 tiers, in which FRF of 1 is applied on the CCUs with lower power, whereas FRF of 3 is used on CMUs with moderate power, and FRF of 9 on CRUs with higher power. In this way, the CRUs become more robust against CCI, but at the expense of a decrease on available bandwidth for the CMUs.

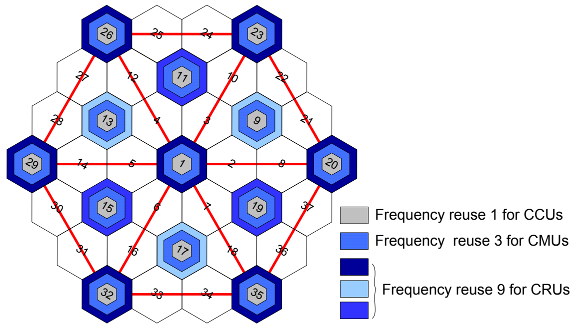

Fig. 3. Concept of the EFFR-A scheme in a cellular system, in which CCUs use reuse-1 subchannels with lower power, CMUs use reuse-3 subchannels with moderate power, and CRUs use reuse-9 subchannels with higher power.

D. *Enhanced Fractional Frequency Reuse – Beyond*

The only difference between the Enhanced Fractional Frequency Reuse - Beyond (EFFR-B) design and the EFFR scheme is that the policy, which is applied on the CRUs in the EFFR-A scheme, are executed to the CEUs in the EFFR scheme. As shown in Fig. 4, the EFFR-B applies reuse-1 for CCUs with lower power, reuse-9 for the residual CEUs with higher power.

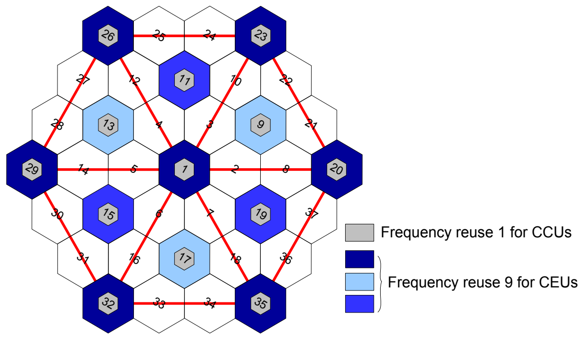

Fig. 4. Concept of the EFFR-B scheme in a cellular system based on FRF of 1 for CCUs and FRF of 9 for the CEUs.

III. CARRIER TO INTERFERENCE COMPUTATION

In this section we will derive Carrier-to-Interference-plus-Noise-Ratio (CINR) for all reuse partitioning schemes mentioned in the last section. In OFDMA based communication networks, resource allocation is based on channel quality of each subchannel. And with the reuse partitioning techniques, subchannel assignment depends on the geographic positions of users. Therefore, in what follows, we are concerned about the received CINR value on each subchannel.

For a theoretical analysis of a reuse-1 cellular system, an investigation on a cell with surrounding interfering cells up to 3 tiers is reasonable and convincing. Fig. 5 instantiates the studied system with 36 adjacent interfering cells and 5 different co-channel distances D_j for $0 \leq j \leq 5$. Table I gives the relation between each reuse distance D_j and cell radius R.

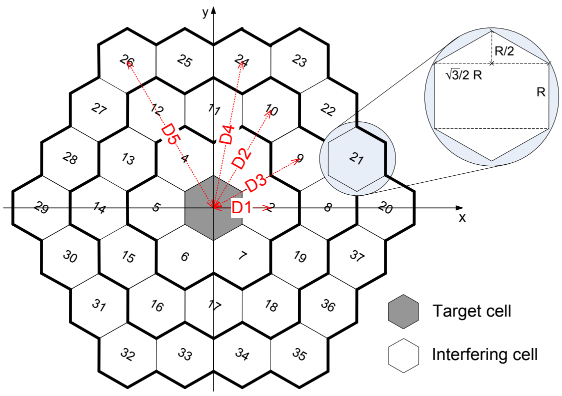

Fig. 5. The evaluation cellular system with interfering cells up to 3 tiers with 5 different co-channel distance: $\boldsymbol{D_1}$, $\boldsymbol{D_2}$, $\boldsymbol{D_3}$, $\boldsymbol{D_4}$ and $\boldsymbol{D_5}$.

We are interested in the CINR values for uplink (UL) traffic at the base station (BS) and for downlink (DL) traffic at user terminals (UT). According to [6], the generally radio propagation can be modeled as

$$P_{Rx\_SCH} = P_{Tx\_SCH} \cdot \left(\frac{c_0}{4\pi f}\right)^2 \cdot g_{Tx} \cdot g_{Rx} \cdot \frac{1}{l^{\gamma}} = \frac{\zeta}{l^{\gamma}} \qquad (1)$$

, where $P_{Tx\text{-}SCH}$ is the transmission power level for one subchannel and $P_{Rx\text{-}SCH}$ the received power on this subchannel, c_0 the speed of light, l the distance between transmitter and receiver, γ a propagation coefficient between 2 and 5, g_{Tx} and g_{Rx} the antenna gains at the receiver and the transmitter side.

Let the BS of the target cell being situated at the grid origin in the Cartesian coordinates as shown in Fig. 5, the received carrier level on a subchannel C_{SCH} at position (x, y) is therefore:

$$C_{SCH}(x,y) = \frac{\zeta_{SCH}}{(\sqrt{x^2+y^2})^{\gamma}} \qquad (2)$$

, where ζ_{SCH} varies depending on the transmission power $P_{Tx\text{-}SCH}$ in accordance with the type of user (CCU, CEU, CMU or CRU) corresponding to each scheme. Equation (2) is also well suited for UL traffic.

TABLE I

RELATIONS BETWEEN D_J, R AND CELL TYPE FOR DIFFERENT TIERS

Tier	D_j	Value	Corresponding cell type	Number of cells for each type
1st	D_1	$\sqrt{3}\cdot R$	A	6
2nd	D_2	$2\sqrt{3}\cdot R$	B	6
2nd	D_3	$3\cdot R$	C	6
3rd	D_4	$\sqrt{21}\cdot R$	D	12
3rd	D_5	$3\sqrt{3}\cdot R$	E	6

In terms of the interference I_{SCH}, since the locations (x_{0i}, y_{0i}) of all BSs in the surrounding interfering cells are fixed, the CCI received by a user located at (x, y) for DL traffic can easily be derived by:

$$I^{DL}_{SCH}(x,y) = \sum_{i=2}^{37} \frac{\zeta_{SCH}}{[d_i(x,y)]^{\gamma}}, \qquad (3)$$

with

$$d_i(x,y) = \sqrt{(x_{0i}-x)^2 + (y_{0i}-y)^2}, \text{ for } 2 \leq i \leq 37 .$$

With the help of the analytical methods described in [9], the mean UL interference I^{UL}_{SCH} yielded by one interfering cell can be calculated by integrating the received power of a point (x, y) over the whole hexagonal cell area.

$$I^{UL}_{SCH} = \frac{\zeta_{SCH}}{cellArea} \cdot \iint_{cellArea} (x^2+y^2)^{-\frac{\gamma}{2}} \qquad (4)$$

According to each type of reuse distance D_j in 3 tiers of surrounding cells, there are 5 types of co-channel cells (Type-A, -B, -C, -D and -E in Table I), which generate CCI to the observed center cell. As indicated in Fig. 5, 5 corresponding mean UL interference ($I^{UL}_{SCH\text{-}A}$, $I^{UL}_{SCH\text{-}B}$, $I^{UL}_{SCH\text{-}C}$, $I^{UL}_{SCH\text{-}D}$ and $I^{UL}_{SCH\text{-}E}$) of different cell types can be attained by using formula (4). Here, we give the mean UL CCI expression $I^{UL}_{SCH\text{-}D}$ for a 3rd-tier interfering cell Nr. 21 of type-D as an example, which depends on two factors ζ_{SCH} and R.

$$\begin{aligned} I^{UL}_{SCH\_D}(\zeta_{SCH}, R) &= \frac{\zeta_{SCH}}{(3/2)\cdot\sqrt{3}\cdot R^2} \\ &\cdot [\int_{2\cdot R}^{\frac{5}{2}R} \int_{\sqrt{3}\cdot y}^{-\sqrt{3}\cdot y+5\cdot\sqrt{3}\cdot R} (x^2+y^2)^{-\frac{\gamma}{2}} dxdy \qquad (4a) \\ &+ \int_{R}^{2\cdot R} \int_{2\cdot\sqrt{3}\cdot R}^{3\cdot\sqrt{3}\cdot R} (x^2+y^2)^{-\frac{\gamma}{2}} dxdy \\ &+ \int_{\frac{R}{2}}^{R} \int_{-\sqrt{3}\cdot y+3\cdot\sqrt{3}\cdot R}^{\sqrt{3}\cdot y+2\cdot\sqrt{3}\cdot R} (x^2+y^2)^{-\frac{\gamma}{2}} dxdy]. \end{aligned}$$

The mean UL CCI of other cell types can be calculated as the same way. Due to the length restriction, we will not present them all in this work.

For any of the studied schemes, the computation formula of received carrier level C_{SCH} for both UL and DL is identical. However, the mean UL CCI formulas for them are different. In the following, we will give the UL CCI equations for the SFR, EFFR, EFFR-A and EFFR-B respectively.

TABLE II

TRANSMISSION POWER FOR ALL STUDIED SCHEMES

Scheme	$P_{Tx\ SCH}$ in UL [mW]			$\sum P_{Tx}$ in UL [mW]	$P_{Tx\ SCH}$ in DL [mW]			$\sum P_{Tx}$ in DL [mW]
Reuse 1	66.67			2000	66.67			2000
Reuse 3	200			2000	200			2000
SFR	CCU	CEU		3333	CCU	CEU		2000
	66.67	200			40	120		
EFFR	CCU	CEU		2000	CCU	CEU		2000
	66.67	200			66.67	200		
EFFR-A	CCU	CMU	CRU	2000	CCU	CMU	CRU	2000
	66.67	200	200		66.67	200	600	
EFFR-B	CCU	CEU		2000	CCU	CEU		2000
	66.67	200			66.67	600		

A. Average Uplink Interference using SFR

The average CCI received by the BS together with the UL traffic from a CEU can be calculated as

$$\begin{aligned} I_{SCH\_CEU}^{UL} &= 6\cdot\left[I_{SCH\_C}^{UL}(\zeta_{CEU},R)-I_{SCH\_C}^{UL}(\zeta_{CEU},R_{CCU})\right] \\ &+6\cdot\left[I_{SCH\_E}^{UL}(\zeta_{CEU},R)-I_{SCH\_E}^{UL}(\zeta_{CEU},R_{CCU})\right] \\ &+6\cdot I_{SCH\_A}^{UL}(\zeta_{CCU},R_{CCU})+6\cdot I_{SCH\_B}^{UL}(\zeta_{CCU},R_{CCU}) \\ &+6\cdot I_{SCH\_D}^{UL}(\zeta_{CCU},R_{CCU}) \end{aligned} \tag{5}$$

, where R_{CCU} defines the range for the CCUs. And the average CCI for UL traffic from a CCU can be reckoned up as

$$\begin{aligned} I_{SCH\_CCU}^{UL} &= 3\cdot\left[I_{SCH\_A}^{UL}(\zeta_{CEU},R)-I_{SCH\_A}^{UL}(\zeta_{CEU},R_{CCU})\right] \\ &+3\cdot\left[I_{SCH\_B}^{UL}(\zeta_{CEU},R)-I_{SCH\_B}^{UL}(\zeta_{CEU},R_{CCU})\right] \\ &+6\cdot\left[I_{SCH\_D}^{UL}(\zeta_{CEU},R)-I_{SCH\_D}^{UL}(\zeta_{CEU},R_{CCU})\right] \\ &+3\cdot I_{SCH\_A}^{UL}(\zeta_{CCU},R_{CCU})+3\cdot I_{SCH\_B}^{UL}(\zeta_{CCU},R_{CCU}) \\ &+6\cdot I_{SCH\_C}^{UL}(\zeta_{CCU},R_{CCU})+6\cdot I_{SCH\_D}^{UL}(\zeta_{CCU},R_{CCU}) \\ &+6\cdot I_{SCH\_E}^{UL}(\zeta_{CCU},R_{CCU}). \end{aligned} \tag{6}$$

B. Average Uplink Interference using EFFR

For the EFFR scheme, the average UL interference generated by the CEUs in the neighboring cells can be calculated as

$$\begin{aligned} I_{SCH\_CEU}^{UL} &= 6\cdot\left[I_{SCH\_C}^{UL}(\zeta_{CEU},R)-I_{SCH\_C}^{UL}(\zeta_{CEU},R_{CCU})\right] \\ &+6\cdot\left[I_{SCH\_E}^{UL}(\zeta_{CEU},R)-I_{SCH\_E}^{UL}(\zeta_{CEU},R_{CCU})\right]. \end{aligned} \tag{7}$$

And the average UL interference caused by the CCUs in the 3 tiers of surrounding cells can be summed up as

$$\begin{aligned} I_{SCH\_CCU}^{UL} &= 6\cdot I_{SCH\_A}^{UL}(\zeta_{CCU},R_{CCU}) \\ &+6\cdot I_{SCH\_B}^{UL}(\zeta_{CCU},R_{CCU})+6\cdot I_{SCH\_C}^{UL}(\zeta_{CCU},R_{CCU}) \\ &+12\cdot I_{SCH\_D}^{UL}(\zeta_{CCU},R_{CCU})+6\cdot I_{SCH\_E}^{UL}(\zeta_{CCU},R_{CCU}). \end{aligned} \tag{8}$$

For the EFFR-A and EFFR-B schemes, the average UL interference $I_{SCH\_CCU}^{UL}$ is as same as which using EFFR scheme. So, in what follow, we will complete the UL CCI formulas at the BS for its receiving packets from other more distant users.

C. Average Uplink Interference using EFFR–A

The average UL interference together with the UL traffic form a CMU can be calculated as

$$\begin{aligned} I_{SCH\_CMU}^{UL} &= 6\cdot\left[I_{SCH\_C}^{UL}(\zeta_{CMU},R_{CMU})-I_{SCH\_C}^{UL}(\zeta_{CMU},R_{CCU})\right] \\ &+6\cdot\left[I_{SCH\_E}^{UL}(\zeta_{CMU},R_{CMU})-I_{SCH\_E}^{UL}(\zeta_{CMU},R_{CCU})\right] \end{aligned} \tag{9}$$

, where R_{CMU} gives the maximum range for the CMUs. The average UL interference yielded by the CRUs in the interfering cells (see Fig. 3) can be computed as

$$I_{SCH\_CRU}^{UL} = 6\cdot\left[I_{SCH\_E}^{UL}(\zeta_{CRU},R)-I_{SCH\_E}^{UL}(\zeta_{CRU},R_{CMU})\right]. \tag{10}$$

D. Average Uplink Interference using EFFR–B

Similar calculation can be taken for the EFFR-B scheme for the CCI resulted by the CEUs in the certain reuse-9 co-channel cells as shown in Fig. 4

$$I_{SCH\_CEU}^{UL} = 6\cdot\left[I_{SCH\_E}^{UL}(\zeta_{CEU},R)-I_{SCH\_E}^{UL}(\zeta_{CEU},R_{CCU})\right]. \tag{11}$$

Now, we can finally accomplish the CINR equation at position (x, y) for the SFR, EFFR, EFFR-B schemes:

$$CINR_{SCH}(x,y)=\begin{cases} \dfrac{C_{SCH\_CEU}(x,y)}{I_{SCH\_CEU}(x,y)+N}, for\sqrt{x^2+y^2}\in[R_{CCU},R] \\ \dfrac{C_{SCH\_CCU}(x,y)}{I_{SCH\_CCU}(x,y)+N}, for\sqrt{x^2+y^2}\in[0,R_{CCU}) \end{cases} \tag{12}$$

, and the CINR equation at position (x, y) for the EFFR-A scheme:

$$CINR_{SCH}(x,y)=\begin{cases} \dfrac{C_{SCH\_CRU}(x,y)}{I_{SCH\_CRU}(x,y)+N}, for\sqrt{x^2+y^2}\in[R_{CMU},R] \\ \dfrac{C_{SCH\_CMU}(x,y)}{I_{SCH\_CMU}(x,y)+N}, for\sqrt{x^2+y^2}\in[R_{CCU},R_{CMU}). \\ \dfrac{C_{SCH\_CCU}(x,y)}{I_{SCH\_CCU}(x,y)+N}, for\sqrt{x^2+y^2}\in[0,R_{CCU}) \end{cases} \tag{13}$$

The CINR equations are applicable for both UL and DL traffic.

IV. Coverage Comparison

Fig. 5 gives the considered cellular scenario which consists of 37 hexagonal cells with central BSs. For the evaluation, antenna gain is neglected at the receiver as well as at the transmitter. 30 subchannels with a bandwidth of 20 MHz are located at 5.47GHz. The minimum receiver requirement for BPSK½ is 6.4 dB which is taken from the 802.16 standard [7]. The maximum transmission power of BSs is restricted to 2000 mW of 33 dBm, and for UTs is 200mW or 23 dBm. Table II details transmission power on a subchannel used by each type of users for all studied schemes.

The suburban C1 Metropol path loss model from the IST – WINNER project [10] was applied in the analysis. The C1 Metropol is a composition of two models, a LOS and a NLOS model. Equation (14) and (15) list their parameters respectively.

$$\text{LOS:} \quad \beta=10^{-\frac{41.9}{10}}=6.457*10^{-5} \qquad \gamma=\frac{23.8}{10}=2.38 \tag{14}$$

$$\text{NLOS:} \quad \beta=10^{-\frac{27.7}{10}}=1.698*10^{-3} \qquad \gamma=\frac{40.2}{10}=4.02 \tag{15}$$

The other main relevant parameters used in simulations are shown in Table III.

TABLE III

Assumptions for Evaluation

Parameter	Value
System bandwidth	20 MHz
Center frequency	5470 MHz
Subcarriers (FFT size)	2048
OFDMA symbol duration	102.858 µs
Number of data subcarriers	1440
Number of subchannels	30
Number of interfering cells	36 (up to 3 tiers)
UT thermal noise density	-174 dBm/Hz
Noise figure at [BS, UT]	[5, 7] dB
Minimum CINR	6.4 dB

In the following, we will compare the coverage of all studied reuse partitioning schemes under LOS and NLOS condition separately. First, the CINR level at the cell border is evaluated with varying cell radius R, so that the maximum cell radius R_{max} for each scheme can be found. Then, with the determined R_{max}, the CINR for a user traversing the cell across the x-axis is given, with which the boundary for partitioning CCUs and CEUs (or CMUs and CRUs) for all in section II mentioned schemes as well as the coverage using each scheme will come out.

A. LOS Condition

Fig. 6a plots the UL CINR perceived at the BS versus the cell radius *R*, while a UT as a transmitter is located at the cell border. And Fig. 6b represents the DL CINR received at the cell border with varying cell radius. Both scenarios are under LOS propagation. The maximum cell radius (CINR of 6.4 dB) is highlighted by stems. In general, the CINR decreases with an increasing cell radius for both UL and DL situations. The both UL and DL CINR using the EFFR-A or -B scheme are better than the other schemes with any cell radius. This is mainly due to the fact that the UTs at the cell border using the EFFR-A or -B work with a large co-channel distance ($D_5 = 3\sqrt{3} \cdot R$). Comparing UL and DL, the DL CINR applying the EFFR-A or -B scheme (see Fig. 6b) is higher than their UL CINR (see Fig. 6a), because in DL the BS may use three times stronger transmission power (600 mW) than the maximum transmission power of a UT (200 mW). However, with the other schemes, the UL CINR seems slight better than the DL CINR. Another phenomenon exposed in both Fig. 6a und Fig. 6b is that besides EFFR-A and EFFR-B schemes, the other schemes do not provide a sufficient CINR level at the cell border for DL or over cell radius for UL under LOS

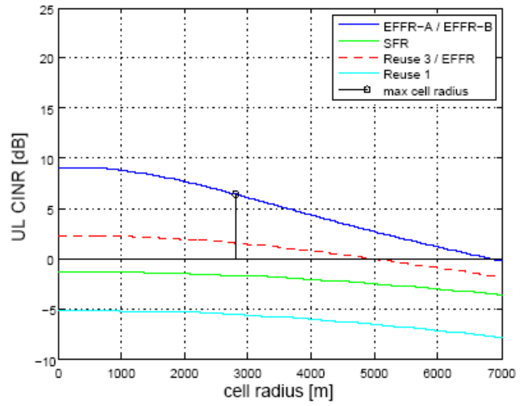

(a)

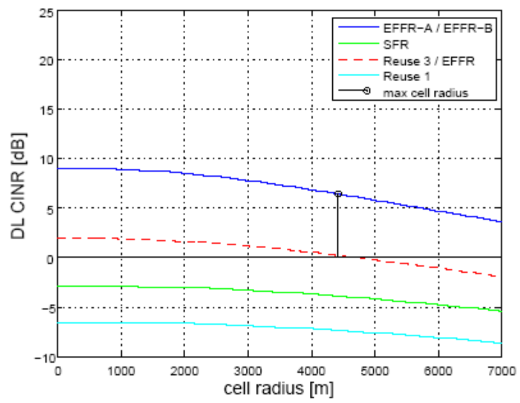

(b)

Fig. 6. CINR versus the cell radius *R* using C1 LOS path loss model: (a) UL CINR perceived at the central BS while a UT as a transmitter located at the cell border; (b) DL CINR received at the cell border.

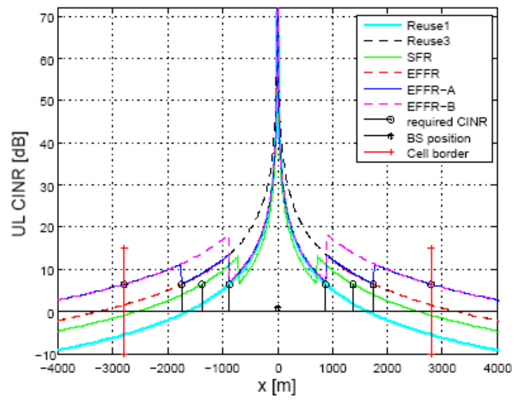

(a) UL CINR received by the BS

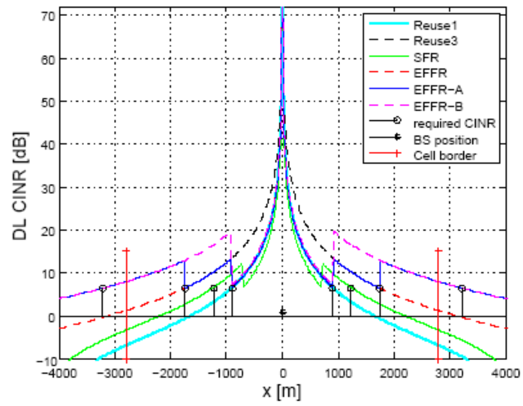

(b) DL CINR received by the UT

Fig. 7. CINR distribution, when a UT traverses the cell with a radius of 2800 m under the C1 LOS propagation.

propagation. Using the EFFR-A or -B scheme, the maximal cell radius reaches 2814 m for UL and 4424 m for DL respectively.

As cell radius for UL and DL should be identical, we choose the minor maximal cell radius 2814 m as cell radius *R* to evaluate the CINR distribution along with varying distance between a UT and the BS. Fig. 7 displays the CINR for a UT traversing the cell across the x-axis for both UL (Fig. 7a) and DL (Fig. 7b) under LOS propagation. The range of coverage of a scheme is marked by two stems, whose height indicates the minimum receiver requirement (6.4 dB) for the PHY mode BPSK½. The CINR by using the EFFR series is better than SFR scheme at any position for both UL and DL. In the figures we can also find the boundary for partitioning CCUs and CEUs (or CMUs and CRUs) for all mentioned reuse partitioning schemes, which is determined by the maximal coverage ranges of the CCUs. The CINR of CCUs by using SFR is worse than the conversional reuse-1 scheme, since the CEUs of some neighboring cells reuse the same resources at the same time with higher transmission power. Though the CINR of the CEUs using SFR is better than which using the reuse-1, it is still worse than the classical reuse-3 scheme. For the reuse-1, reuse-3 and EFFR, their coverage for UL is quite similar to the DL coverage. On the contrary, the SFR can reach maximum 1232m from the BS for DL (see Fig. 7b), but 1736m for UL (see Fig. 7a). This is because the transmission power on each subchannel for DL is smaller than that for UL (see Table II). As a result, SFR can cover 24% of the cell for

UL, but 19% of the cell for DL. Among all schemes, only the EFFR-A or -B scheme has the capability of serving the whole cell under LOS propagation. For DL, they even can provide a CINR higher than 6.4 dB at the cell border (see Fig. 7b).

B. NLOS Condition

Fig. 8 and Fig. 9 show the comparable results under NLOS propagation, where the path loss coefficient γ is nearly two times higher than under LOS propagation (see Equation (15)).

Comparing Fig. 8 and Fig. 6, the CINR under NLOS propagation at small radii is higher than which with LOS, as the CCI is substantially reduced caused by the bigger path loss coefficient γ. Besides the EFFR-A or -B scheme, the reuse-3 and the EFFR scheme also allow for cell radii of 270 m for UL (see Fig. 8a) and 248 m for DL (see Fig. 8b) in a NLOS scenario. Nevertheless, applying EFFR-A or –B scheme the larger maximal cell radii can be attained, namely, 298 m for UL and 391m for DL. And the SFR scheme and the reuse-1 scheme can still not provide a sufficient CINR for both UL and DL. Similar to LOS results as shown in Fig. 6, other than the EFFR-A or –B scheme, the UL CINR over the cell radius *R* is higher than the DL CINR with the other schemes. This is because in UL the receiver is located at the center of the cell and not at the border, which reduces the received interference.

Like the Fig. 7, Fig. 9 shows CINR distribution for both UL and DL under NLOS propagation for a UT traversing across the cell, where the smaller UL maximal cell radius of

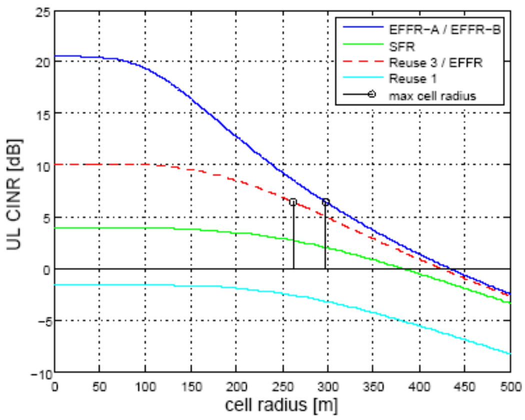

(a)

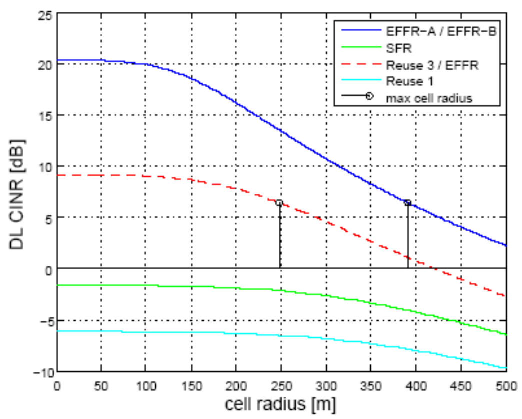

(b)

Fig. 8. CINR versus the cell radius *R* using C1 NLOS path loss model: (a) UL CINR perceived at the central BS while a UT as a transmitter located at the cell border; (b) DL CINR received at the cell border

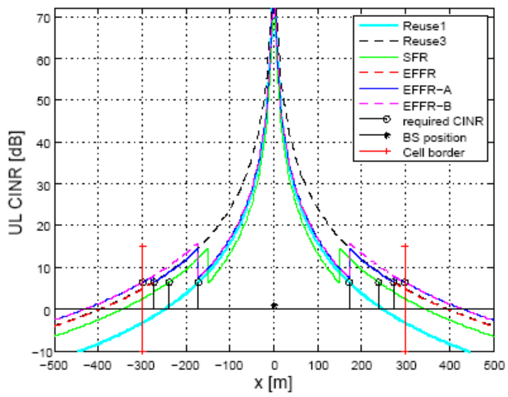

(a) UL CINR received by the BS

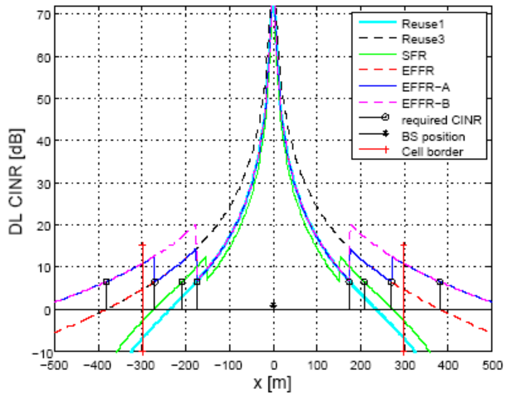

(b) DL CINR received by the UT

Fig. 9. CINR distribution when a UT traverses the cell with a radius of 298 m under the C1 NLOS propagation.

the EFFR-A scheme (298m) is chosen as a cell radius for evaluation. Fig. 9 exhibits similar features as which in Fig. 7. Moreover, either LOS or NLOS, the CINR using the classical reuse schemes or SFR for DL decays always rapidly than which for UL, which means the DL CCI by using those schemes is severer than the UL CCI.

V. MEAN CELL CAPACITY COMPUTATION

The subchannel data throughput (see Table IV) at a certain position $Thr_{SCH}(x,y)$ can be derived by the perceived CINR for each Modulation and Coding Scheme (MCS) in the scenario as described in Table III. We use the seven different PHY modes and their corresponding CINR measures from the air interfaces of IEEE 802.16e-2004 [7].

TABLE IV

PHY MODES AND CORRESPONDING SUBCHANNEL THROUGHPUT

Modulation	Coding rate	Min. receiver CINR [dB]	PHY Throughput per subchannel [Mb/s]
BPSK	1/2	6.4	0.233
QPSK	1/2	9.4	0.467
QPSK	3/4	11.2	0.7
16QAM	1/2	16.4	0.933
16QAM	3/4	18.2	1.4
64QAM	2/3	22.7	1.867
64QAM	3/4	24.4	2.1

In the next step, the average subchannel throughput $Thr_{SCH\text{-}avg}$ can be obtained by integrating the $Thr_{SCH}(x,y)$ over the entire cell and dividing it by the cell area [8]. In the end, we calculate the mean cell capacity *CAP* by multiplying the $Thr_{SCH\text{-}avg}$ by the number of available subchannls. As the number of available subchannels is different for each scheme, and the EFFR series calculates the $Thr_{SCH\text{-}avg}$ differently for different zone-type of users, in what follows we give the calculations for all studied schemes separately.

A. SFR Scheme and Classical Reuse Schemes

The average subchannel throughput for classical reuse schemes and the SFR scheme is represented as

$$Thr_{SCH\_avg} = \frac{\iint_{cellArea} Thr_{SCH}(x,y)dxdy}{cellArea}. \tag{16}$$

The whole bandwidth, which means all 30 subchannels (see Table III) in the system, are available for the SFR and the reuse-1 scheme, whereas just one third of the bandwidth 10 subchannels can be used by the reuse-3 scheme.

$$\begin{cases} CAP^{SFR} = Thr_{SCH\_avg}^{SFR} \cdot 30 \\ CAP^{reuse-1} = Thr_{SCH\_avg}^{reuse-1} \cdot 30 \\ CAP^{reuse-3} = Thr_{SCH\_avg}^{reuse-3} \cdot 10 \end{cases} \tag{17}$$

B. EFFR Scheme

Using the EFFR series, the subchannel allocation depends on the certain zone of a user. So, according to different zone-types of the users we give their average subchannel throughput separately. For the CEUs

$$Thr_{SCH\_avg\_CEU}^{EFFR} = \frac{1}{cellArea - CCUArea} \cdot \left(\iint_{cellArea} Thr_{SCH\_CEU}^{EFFR}(x,y)dxdy - \iint_{CCUArea} Thr_{SCH\_CEU}^{EFFR}(x,y)dxdy \right), \tag{18)}$$

and for the CCUs

$$Thr_{SCH\_avg\_CCU}^{EFFR} = \frac{\iint_{CCUArea} Thr_{SCH\_CCU}^{EFFR}(x,y)dxdy}{CCUArea}. \tag{19}$$

Finally, the mean cell capacity can be calculated as

$$CAP^{EFFR} = M \cdot Thr_{SCH\_avg\_CEU}^{EFFR} + 3 \cdot N \cdot Thr_{SCH\_avg\_CCU}^{EFFR} \tag{20}$$

, where *M* denotes the available subchannels for CEUs and *3N* for CCUs. In addition, they are subjected to the constraints that $0 < N < 10$ and $M + N = 10$ which is the number of subchannels for the Primary Segment. *N* should not be zero, as that means it is impossible for CCUs to get any resources. $N = 10$ means $M = 0$, which is also unsuitable, since the CEUs would therewith never have chance to be served.

C. EFFR–A Scheme

Calculation of $Thr_{SCH\_avg\_CCU}^{EFFR-A}$ should be as same as that in EFFR scheme. The average subchannel throughput for the CMUs and CRUs are similar to the $Thr_{SCH\_avg\_CEU}^{EFFR}$, however, not same

$$Thr_{SCH\_avg\_CMU}^{EFFR-A} = \frac{1}{CMUArea - CCUArea} \cdot \left(\iint_{CMUArea} Thr_{SCH\_CMU}^{EFFR-A}(x,y)dxdy - \iint_{CCUArea} Thr_{SCH\_CMU}^{EFFR-A}(x,y)dxdy \right), \tag{21}$$

and

$$Thr_{SCH\_avg\_CRU}^{EFFR-A} = \frac{1}{cellArea - CMUArea} \cdot \left(\iint_{cellArea} Thr_{SCH\_CRU}^{EFFR-A}(x,y)dxdy - \iint_{CMUArea} Thr_{SCH\_CRU}^{EFFR-A}(x,y)dxdy \right). \tag{22}$$

The mean cell capacity for the EFFR-A scheme is

$$CAP^{EFFR-A} = M_2 \cdot Thr_{SCH\_avg\_CRU}^{EFFR-A} + M_1 \cdot Thr_{SCH\_avg\_CMU}^{EFFR-A} + 3 \cdot N \cdot Thr_{SCH\_avg\_CCU}^{EFFR-A} \tag{23}$$

, where M_1 and M_2 are the available resue-3 subchannels for CMUs and available reuse-9 subchannels for CRUs respectively. Likewise, they are subjected to the constraints

$$\begin{cases} 0 < N < 10 \\ 0 < M_2 < 3 \\ 3 \cdot M_2 + M_1 + N = 10 \end{cases}$$

With $M_2 = 0$, the EFFR-A scheme is just the EFFR scheme. And the EFFR-A scheme is equal to the EFFR-B scheme, if $M_2 = 3$.

D. EFFR–B Scheme

$Thr_{SCH\_avg\_CEU}^{EFFR-B}$ and $Thr_{SCH\_avg\_CCU}^{EFFR-B}$ can be calculated just as same as which in the EFFR scheme. But the mean cell capacity should be reckoned up as

$$CAP^{EFFR-B} = M_2 \cdot Thr_{SCH\_avg\_CEU}^{EFFR-B} + 3 \cdot N \cdot Thr_{SCH\_avg\_CCU}^{EFFR-B} \tag{24}$$

, where M_2 and *N* must be conformed to the constraints $N > 0$ and $3 \cdot M_2 + N = 10$.

VI. Cell Capacity Comparison

As the performance of EFFR series depends strongly on the *N* and *M* combination, the numerical results for the mean cell capacity versus the number of reuse-1 subchannels *N* will be displayed for all studied schemes under both LOS and NLOS conditions.

A. LOS Condition

Under LOS propagation, the SFR scheme outperforms the conventional reuse-1 and resue-3 schemes for both UL (see Fig. 10a) and DL (see Fig. 10b). But the improvement is limited. Using the EFFR series, they never perform worse than the SFR and the conventional reuse schemes with any value of *N*. With an increasing number of subchannels for the CCUs *N*, the enhancement becomes more and more remarkable, however, at the cost of sacrificing resources for the other users in a cell. This is because CCUs are close to the BS, so they can always get high quality of CINR, and thereby use high grade PHY mode to transmit. Hence, a tradeoff between capacity maximization and fairness should be made. Fig. 10 shows that all EFFR schemes reach similar gains. Nevertheless, together with the results from the Fig. 7 in section IV, only the EFFR-A and EFFR-B schemes can provide 100% coverage. And the EFFR-A with $M_2 = 1$ always performs slightly better than the EFFR. As a consequence, the EFFR-A scheme with $M_2 = 1$ is the best solution for CCI mitigation among all studied schemes in a cellular LOS scenario.

B. NLOS Condition

Fig. 11 displays the mean reachable cell capacities of all studied schemes under NLOS propagation. In UL as shown in

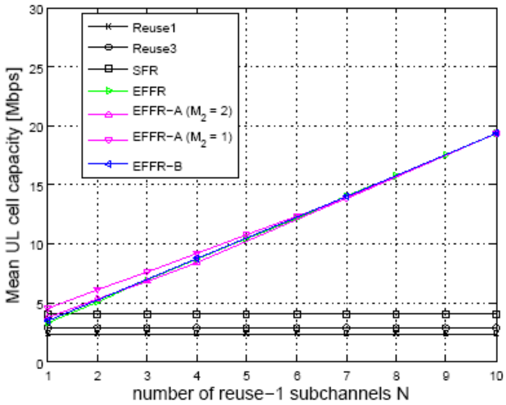

(a) Mean UL cell capacity

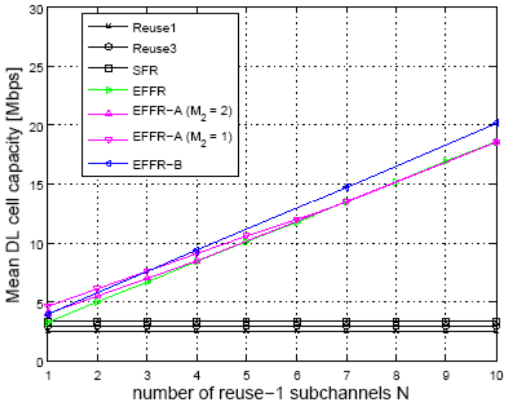

(b) Mean DL cell capacity

Fig. 10. Mean cell capacity under the C1 LOS propagation, having the same environment as in Fig. 7.

Fig. 11a, the SFR surpasses the conventional reuse schemes significantly, whereas it performs quite similar to the reuse-1 scheme in DL (see Fig. 11b). Nevertheless, this doesn't mean that the SFR performs better in UL, because the total system transmission power using SFR is much higher than the other schemes as exhibited in Tabl e II. The EFFR series outperforms the other schemes, when $N \geq 5$ in UL and $N \geq 4$ in DL respectively. In both UL and DL, the EFFR performs slight better than the EFFR-A and EFFR-B schemes. However, in consideration of the coverage as shown in Fig. 9, the EFFR cannot provide 100% coverage, but the EFFR-A and EFFR-B do. Furthermore, the EFFR-A with $M_2 = 1$ is the second best among the EFFR series. So, with a comprehensive consideration of cell coverage and mean reachable cell capacity, the EFFR-A with $N \geq 5$ and $M_2 = 1$ combination is still the best way to alleviate CCI in a cellular NLOS scenario.

VII. Conclusion

In this work, we presented an analytical investigation on reuse partitioning techniques, which are proposed to mitigate CCI in OFDMA-based cellular networks. With CINR calculations, the reasonable boundary definitions for division different user-type zones by using each reuse partitioning scheme can be determined individually. Furthermore, through numerical evaluations, the cell coverage and the mean cell capacity of all studied reuse techniques are presented. The results show that significant coverage gains and cell capacity improvements can be achieved by applying the novel EFFR

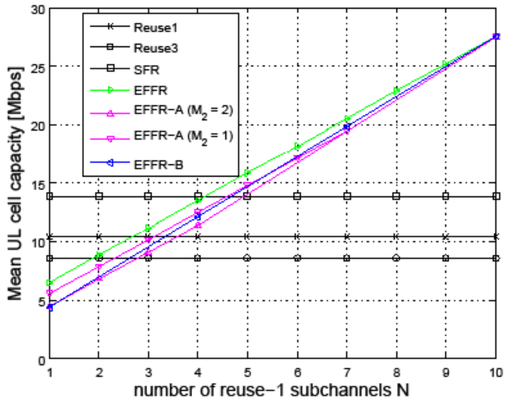

(a) Mean UL cell capacity

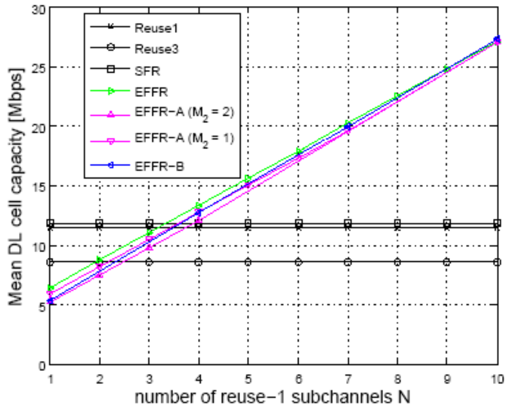

(b) Mean DL cell capacity

Fig. 11. Mean cell capacity under the C1 NLOS propagation, having the same environment as in Fig. 9.

schemes with adequate resource allocations.

References

[1] S. W. Halpern, "Reuse partitioning in cellular systems," in Proceeding IEEE Vehicular Technology Conference, May 1983, vol. 3, pp. 322-327.

[2] 3GPP; Huawei, "Soft frequency reuse scheme for UTRAN LTE", R1-050507, May 2005.

[3] K. T. Kim, S. K. Oh, "An Incremental Frequency Reuse Scheme for an OFDMA Cellular System and Its Performance," in Proc. of the 67th IEEE Vehicular Technology Conference (VTC-Spring 08), May 2008.

[4] Y. Xiang, J. Luo, "Inter-cell interference mitigation through flexible resource reuse in OFDMA based communication networks," in Proc. of the 13th European Wireless Conference (EW2007), Paris, France, April 2007.

[5] Z. Xie and B. Walke, "Frequency Reuse Techniques for Attaining both Coverage and High Spectral Efficiency in OFDMA Cellular Systems," in IEEE Wireless Communications & Networking Conference (WCNC2010), Sydney, Australia, April 2010.

[6] B. Walke, *Mobile Radio Networks – Networking Protocols*. John Wiley & Sons, 2002.

[7] IEEE 802.16-2004, " IEEE standard for local and metropolitan area networks-Part 16: Air interface for fixed broadband wireless access systems," Oct. 1, 2004

[8] J. Habetha and J. Wiegert, "Network Capacity Optimization, Part I: Cellular Radio Networks," in 10th Symposium on Signal Theory, Aachen, Sep 2001, pp.125 – 132.

[9] C. Hoymann, and S. Goebbels, "Dimensioning Cellular WiMAX – Part I: Singlehop Networks," in Proceedings of 13th European Wireless Conference (EW2007), Paris, France, April 2007.

[10] IST-WINNER, "D5.4, Final Report on Link Level and System Level Channel Model," IST-4-027756 WINNER II," Deliverable, September 2006.